Electro-Spark Deposition Coatings for High Temperature Oxidation Resistance

Zhengwei Li [1,2], Wei Gao[1*], Puiming Kwok[1], Sean Li[1] and Yedong He[2]

[1] *Department of Chemical & Materials Engineering*
The University of Auckland, New Zealand
[2] *Department of Surface Science and Corrosion Engineering*
University of Science and Technology Beijing, China

(Received March 7, 2000; final form April 25, 2000)

ABSTRACT

A simple but efficient technique has been developed to produce surface coatings on metals and alloys. This technique uses direct high frequency electrical sparks to melt and deposit metal or alloy coatings onto substrate surface. The present paper reports Al and FeCrAl coatings on AISI 304, 310 and 430 stainless steel and Inconel 600 substrates. Isothermal oxidation in air indicated that the oxidation rates of the coated specimens were much lower than that of the un-coated specimens. The scale spallation resistance was also dramatically improved. The phases and microstructures of the coatings and oxide scales were characterised using XRD and HRSEM. The properties of the different coatings were compared; and the effects of the processing parameters were discussed based on the experimental results. Further improvements in an effort to obtain thicker and more uniform coatings with better oxidation resistance and to use this technique in industrial applications were also proposed.

KEY WORDS:

electro-spark deposition; Al and FeCrAl coatings; 304, 310 and 430 stainless steels; Inconel 600 alloy; oxidation

* Corresponding author, e-mail: w.gao@auckland.ac.nz

1. INTRODUCTION

Good mechanical properties and oxidation resistance are the basis for the industrial applications of high-temperature materials. Unfortunately, these two aspects often conflict with each other. For this reason oxidation protective coatings are extensively used and further developed for full exploitation of the alloy capabilities at high service temperatures. Furthermore, it should be emphasised that the coatings and substrates must be considered as an integrated system. From this viewpoint, if the coating was formed through partial mixing with the substrate, superior properties may be obtained.

Various techniques have been developed to produce high temperature coatings. Generally, these methods can be classified as galvanising, immersing, spraying, cladding and crystallising /1/. However, development of simple and efficient coating methods is a general tendency. The technique of electro-spark deposition is a relatively simple, high-efficient and inexpensive method for surface coating and modification of metals and alloys. Electro-spark deposition is also known as electrical spark toughening, electrical spark alloying, pulsed fusion surfacing and pulsed electrode surfacing. Initially, this method was developed for steel surface hardening /2-4/. Wear-resistant surfaces produced by this technique have been used in industrial applications.

He *et al.* /5,6/ further developed this technique and successfully used it to produce oxidation resistant coatings on a variety of metals and alloys.

The basic principle of the electro-spark deposition is simple /7/. The electrode (serving as the coating/ hardening material) is connected to the positive pole of a specially designed resistance-capacitance (RC) pulse power device. The substrate to be coated is connected to the negative pole. When two electrodes move to each other and come into a certain distance (or touch together), spark discharge takes place and releases the energy stored in the capacitor. The discharging time is so short (1–10,000 μs) that the energy released produces a high temperature (5,000–10,000K), resulting in partial melting of the electrode and substrate surface. The molten materials are mixed together and solidify rapidly, forming an alloying coating layer. This technique can be used to build any electrically conducting coatings onto any conducting substrates.

In the present study, Al and FeCrAl (with or without Y_2O_3 nano-size particles) coatings were deposited onto substrates of AISI 304, 310 and 430 stainless steels and Inconel 600 high temperature alloy. It is well known that additions of a small amount of reactive element oxides can significantly improve the oxidation resistance of FeCrAl alloys /8/. Our results showed that both oxidation and scale spallation resistance have been dramatically improved.

1. EXPERIMENTAL PROCEDURES

2.1. Apparatus

The principal design of the electro-spark generator was sketched in Fig.1 and described in a previous paper /6/. The main difference between the traditional and the present designs is the use of a rotation wheel with a number of teeth as the electrode, greatly increasing the contact frequency of the electrodes. The switching between charging and discharging was realised by the rotation of electrode. The discharging frequency is controlled by adjusting the number of teeth and rotation speed. Additionally, the smoothness of the coating surface is improved due to the abrading effects of the rotating wheel. The operation parameters used in the present work were input voltage = ~70 V, resistance = 3.4 or 6.8 Ω, capacitance = 16.5, 33, or 66 μF, and rotation speed = 17 – 34 r/sec.

2.2. Deposition process

Commercial AISI 304, 310 and 430 stainless steels and Inconel 600 alloy were selected as the substrates due to their industrial importance. The electrode materials are pure Al (>99.8%) and Fe-25Cr-5Al wire (ϕ0.5mm). Fine Y_2O_3 (99.9%) powders were also used for producing oxide dispersed FeCrAl coatings. About 2mg/cm^2 Y_2O_3 powders were applied on the alloy

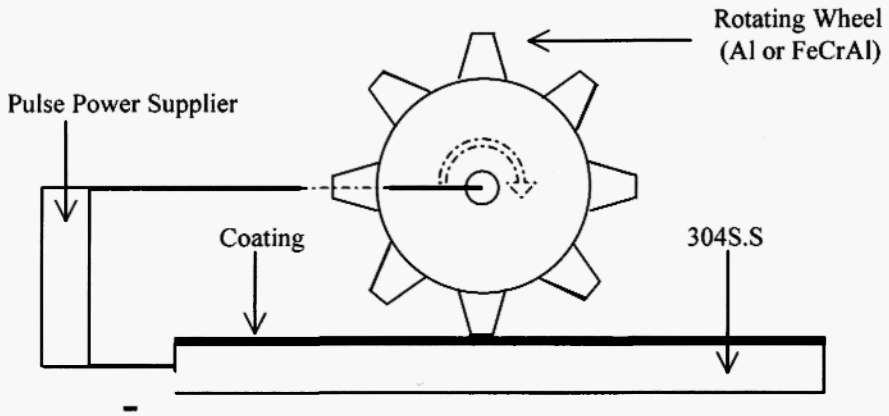

Fig. 1: Schematic of the electro-spark deposition apparatus

Table 1
Nominal composition of the materials used (wt.%)

	Fe	Cr	Ni	Al	Mn	Si
304S.S	bal	18.0-20.0	8.0-10.6	-	2.0	1.0
310S.S	bal	24.0-26.0	19.0-22.0	-	2.0	1.5
430S.S	bal	16.0-18.0	-	-	1.0	1.0
Inconel 600	8.0	15.5	bal			
FeCrAl	bal	23.0-27.0	-	4.5-6.5	-	-

surface, but only a small proportion of these was incorporated into the coatings. The nominal compositions of all materials used are listed in Table.1. Al plates 2-3 mm thick were machined into wheels of ϕ30 mm with 20 teeth. FeCrAl wire was used to wind on a disk with 20 contact points at the edge. The specimens to be coated were ground to 1200 grit SiC paper followed by washing and drying. Normally, the electro-spark deposition was conducted twice for each surface. The first run used a relatively high energy (~0.13 J/per discharge as calculated), the second used a low energy (~0.067 J/per discharge).

2.3. Oxidation kinetics and product characterisation

Oxidation tests were carried out in air in a horizontal tube furnace. After a period of exposure, specimens were withdrawn from the furnace, cooled down in a desiccator for 20 min. The mass gains of the specimens were measured using an electronic-balance with an accuracy of 10 μg. Surface morphologies of the coatings, oxides and polished cross-sections were characterised using a HRSEM (Phillips XL30 FEG) with an EDS attachment. X-ray diffraction was conducted in a Phillips X-ray diffractometer with Co-Kα radiation.

2. RESULTS

3.1 Coatings

Fig.2 represents a typical cross-section of Al coatings on 304 stainless steel produced by the electro-spark deposition technique. The coatings generally cover all specimen surfaces, with a thickness varying between 8 to 16 μm. There are no gaps or pores in the coating or between the coating and substrate, indicating a good adherence. Under an optical microscope, evidence of melting and rapid solidification could be seen on the surface, especially for the Al coatings. The micrograph in Fig.2 shows a multi-phase microstructure, with the light phase containing more Al than the dark phase. Micro-cracks were observed on the surface of Al coatings, which were probably caused by the fast solidification process. FeCrAl coatings appeared to be smoother and more uniform than the Al coatings.

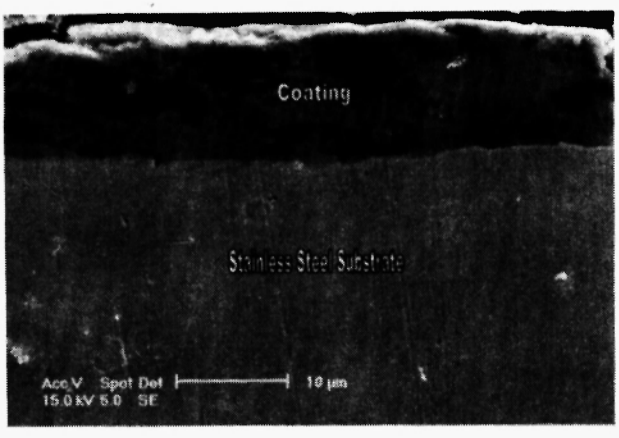

Fig. 2: A typical cross-section SEM image of the coating produced by electro-spark deposition technique

3.2 Oxidation kinetics

Isothermal oxidation kinetics for un-coated and coated 304S.S with Al and FeCrAl (with and without addition of nano-size Y_2O_3 particles) at 1000°C, 310S.S with FeCrAl+Y_2O_3 at 1100°C and 430S.S with Al at 900°C, are presented in Fig.3. Oxidation kinetics of

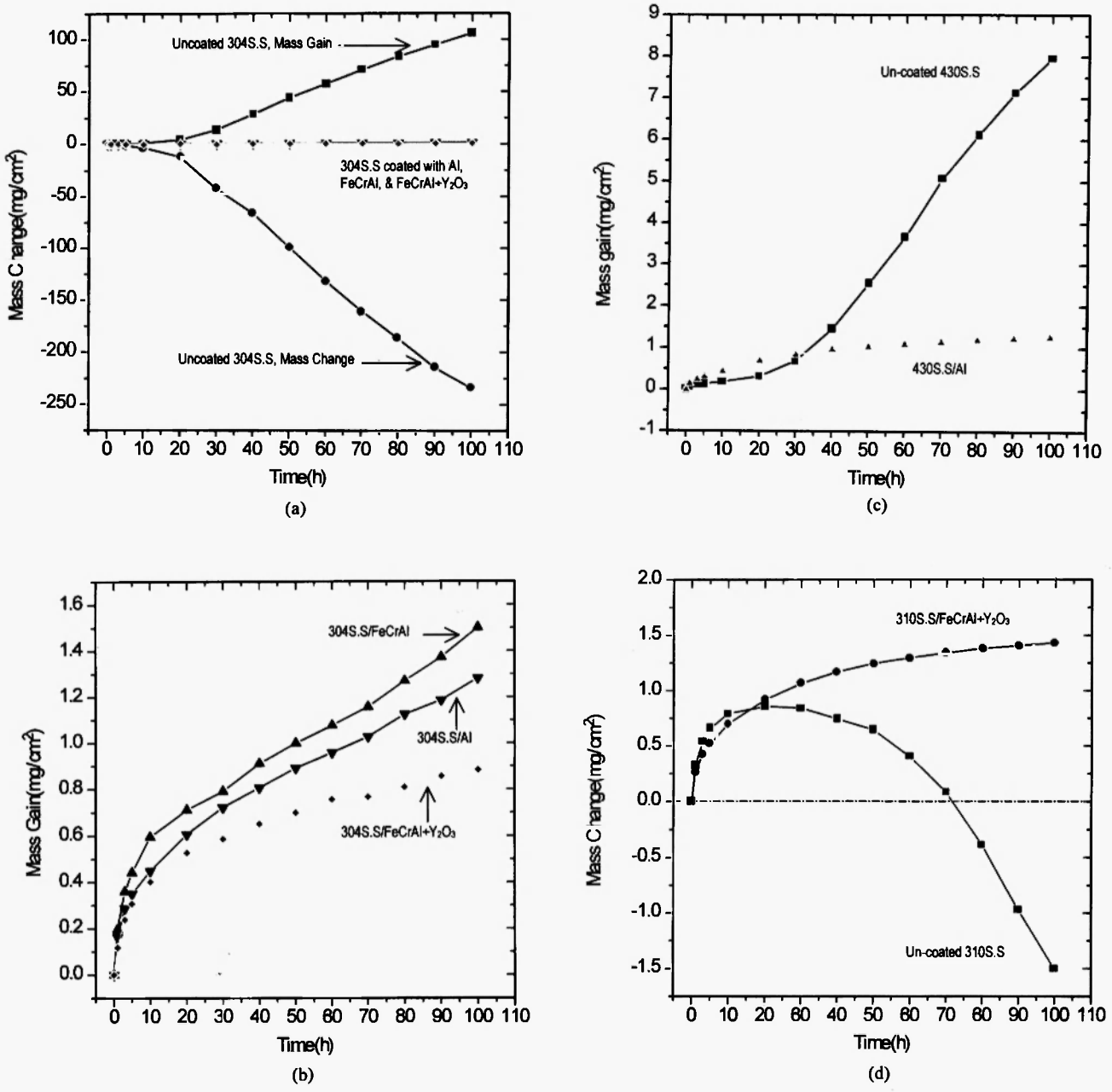

Fig. 3: Oxidation kinetics of uncoated and coated stainless steels in air: (a, b) 304S.S and 304S.S coated with Al or FeCrAl (Y_2O_3) at 1000°C; (c) 430S.S and 430S.S coated with Al at 900°C; and (d) 310S.S and 310S.S coated with FeCrAl + Y_2O_3 at 1100°C

un-coated and coated Inconel 600 with Al at 1000°C are shown in Fig.4.

As can be seen in Fig.3 (a) and (b), severe spallation of oxide scales took place on the surface of un-coated 304S.S specimens (only after 5h oxidation). Mass of the specimen decreased linearly during the testing period, showing the non-protective oxidation behaviour, with the mass loss reaching ~250 mg/cm^2 in 100h. By comparison, the oxidation kinetics of coated specimens obeyed an approximately parabolic rate law, with no obvious spallation observable during the whole testing time. Even though the kinetic curve of 304S.S specimen

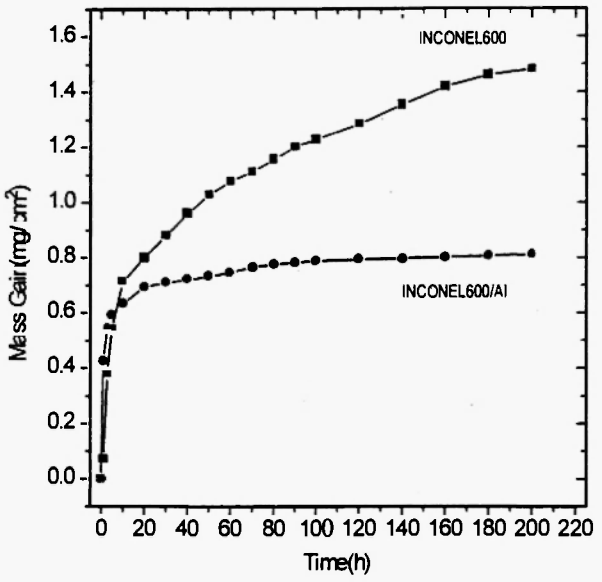

Fig. 4: Oxidation kinetics of Inconel 600 and Inconel 600 coated with Al at 1000°C in air

coated with FeCrAl slowly increased to a linear law after 80h of oxidation (possibly resulting from the degradation of the coatings), the total mass gain was only ~1.5mg/cm^2 after 100h. The mass gains of 304S.S specimens coated with Y_2O_3 dispersed FeCrAl were about 1/2 of that without Y_2O_3. The oxidation kinetics of the un-coated 310S.S in the first 10h obeyed a parabolic rate law, after which the mass of the specimen decreased slowly – evidence of scale spallation – whereas the kinetics of the coated 310S.S followed an approximately parabolic rate law during the whole testing time. The transition from protective to breakaway oxidation could be clearly observed from the oxidation kinetics of the un-coated 430S.S at 900°C, while this transition did not occur for the Al coated 430SS, and its oxidation rate was relatively low.

Oxidation kinetics of Inconel 600 at 1000°C in air obeyed an approximately parabolic rate law for the whole exposure time. After 200h of oxidation, the mass gain reached about 1.5 mg/cm^2. The kinetics of Inconel 600 coated with Al, however, was quite different, showing a fast progress at the initial stage but levelling off after ~10h exposure, evidence of the formation of a stable, protective scale. The total mass gain after 200h of oxidation was only 0.80 mg/cm^2, about a half of the uncoated alloy.

3.3 XRD patterns and oxide phases

The XRD patterns of the un-coated and coated stainless steels and Inconel 600 alloy specimens after oxidation are shown in Figs. 5 and 6, respectively. The oxide phases formed are complex as marked on the peaks. Comparing, e.g. 304S.S with 304S.S coated with Al, it can be seen that $FeCr_2O_4$ and Cr_2O_3 formed in both cases. However, Al_2O_3 peaks appeared in the scales on Al coated alloys, and Cr_2O_3 diffractions are stronger for the coated samples (Fig. 5a). It should be noted that the XRD analysis of the un-coated 304S.S represents only the oxides remained on the surface due to serious scale spallation. As for the un-coated 430S.S, the XRD scanning was run on the higher planeside, showing mainly iron oxides.

3.4. Surface and cross-section morphologies

Figs. 7 and 8 show the surface morphologies and polished cross-sections of the un-coated and coated stainless steels and Inconel 600 alloy after oxidation.

3.4.1. Un-coated and coated 304S.S

It can be clearly seen that serious scale spallation took place on the un-coated 304S.S specimen, Fig. 7 (a). Actually, almost a whole layer of scale detached from the surface during every cooling cycle. The thickness of the specimen was only about a half of the original after 100h oxidation. The polished cross-section shows a non-uniform and porous scale, Fig. 7 (b), evidence of the non-protective nature. The surface of 304S.S coated with Al was basically covered with spinelle-type oxides. Micro-cracks and creep feature on the oxide scale could be observed, Fig. 7 (c). The polished cross-section shows that a continuous oxide scale was formed. Although this scale appears non-uniform (5 to 10 μm thick), it was much denser than that formed on the un-coated specimen. EDS analysis showed the existence of Cr, Al, Fe and O. Cavities were detected along the interface between the scale and substrate. Al_2O_3 and a small amount of SiO_2 internal precipitates could also be observed at some locations along the interface, Fig. 7 (d). The surface of 304S.S coated with Fe-25Cr-5Al after 100h of oxidation was shown as a scale consisting of fine oxide grains. Fig. 7 (e). These grains tend to

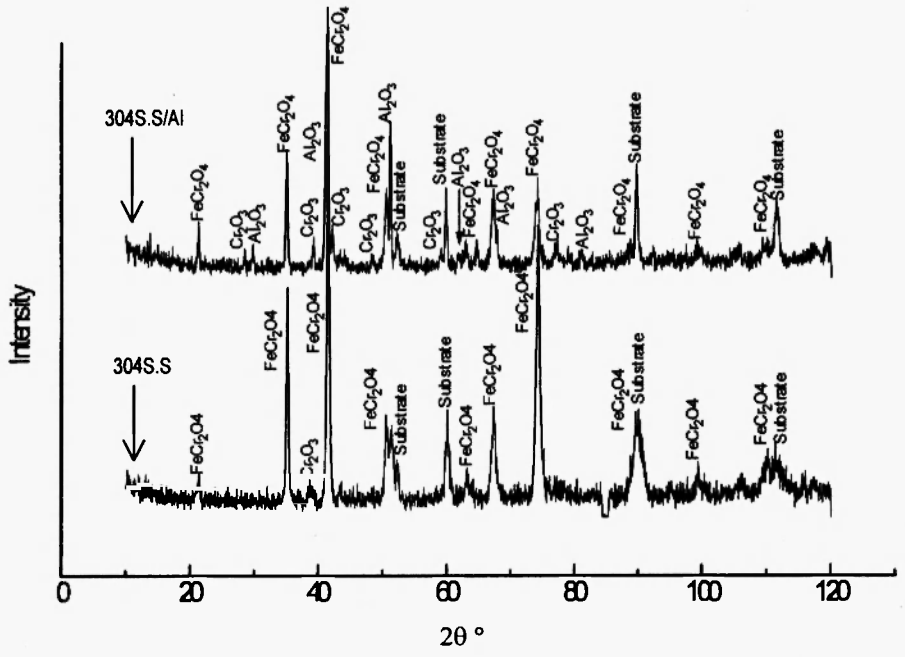

(a)

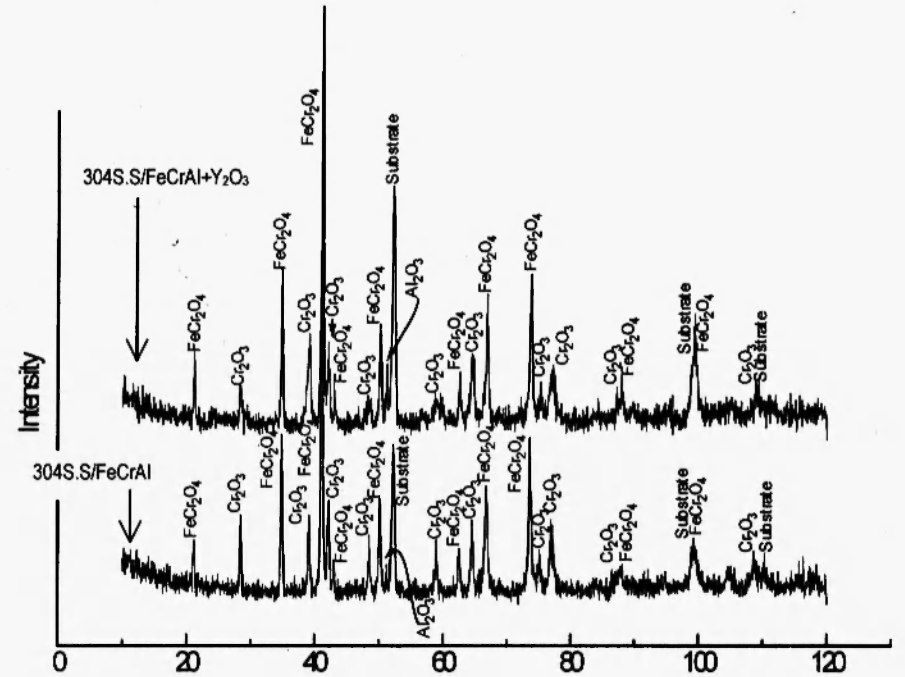

(b)

Fig. 5: XRD patterns of un-coated and coated stainless steel specimens after oxidation: (a) 304S.S and 304S.S/Al; (b) 304S.S/FeCrAl and 304S.S/FeCrAl+Y_2O_3; (c) 430S.S and 430S.S/Al; and (d) 310S.S and 310S.S/FeCrAl+Y_2O_3

Fig 5. continued

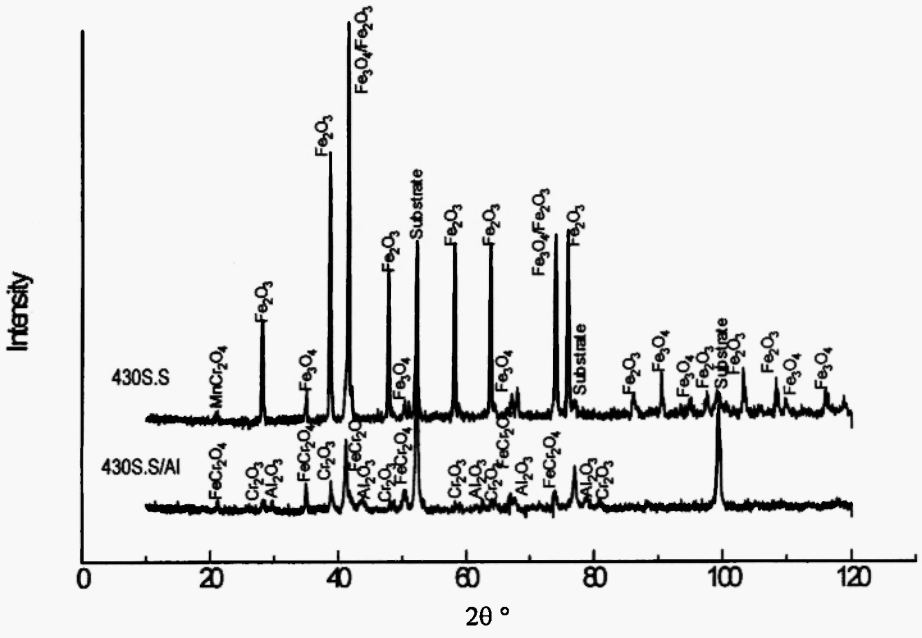

(c)

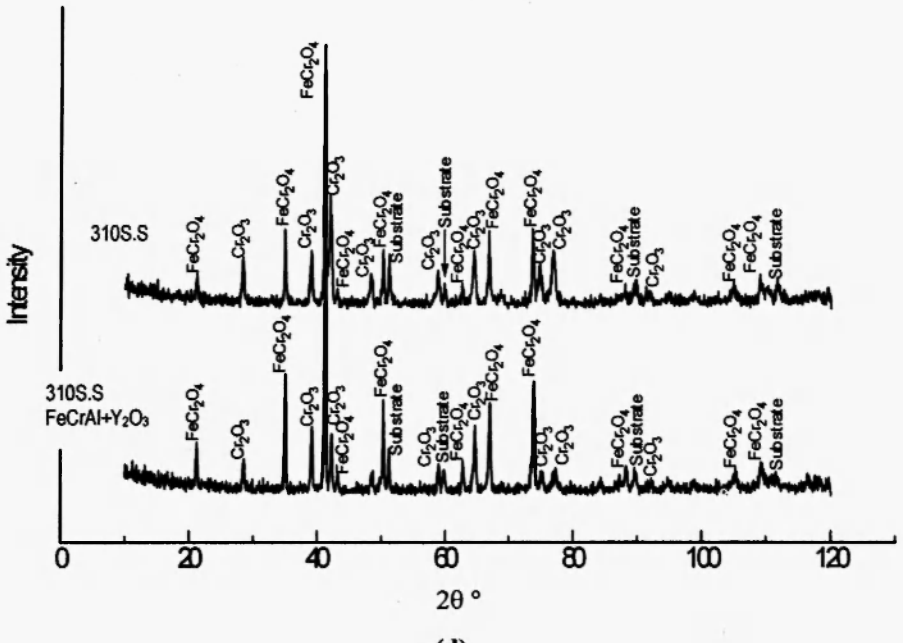

(d)

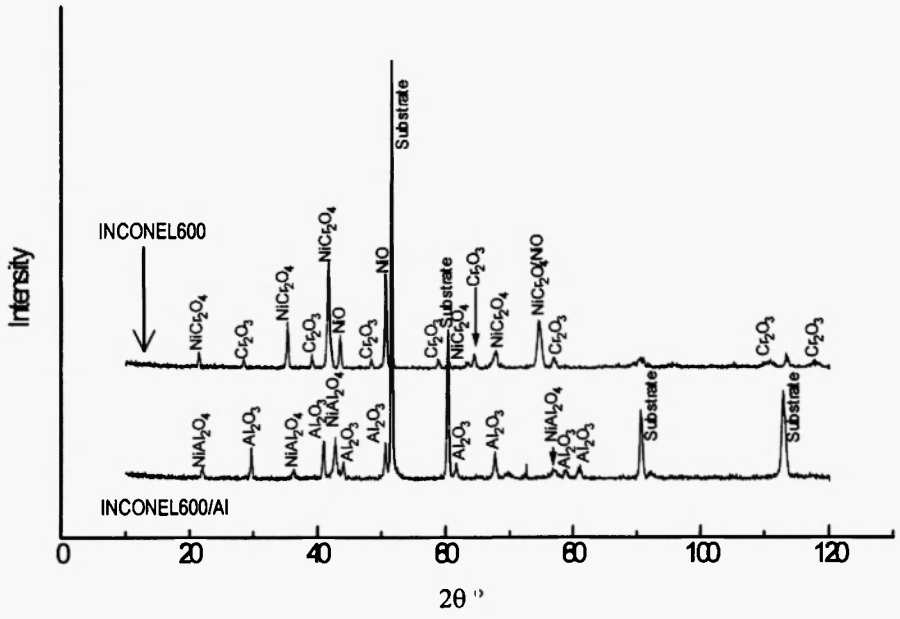

Fig. 6: XRD patterns of un-coated and coated Inconel 600 specimens after oxidation

form large agglomerations. Micro-cracks could be observed on the surface of the oxide scale. A continuous but non-uniform oxide scale with a thickness of ~10μm was shown in the cross-section, Fig.7 (f). Cr, O and small amounts of Al and Fe were detected with EDS analysis. Strips of agglomerate oxides could be observed on a quite uniform oxide scale formed on the surface of 304S.S specimen coated with Fe-25Cr-5Al and nano-sized Y_2O_3 particles. High magnification images revealed that the oxide grains are small, Fig.7 (g). The polished cross-section shows a relatively uniform oxide scale of ~5 μm thick, Fig.7 (h). EDS

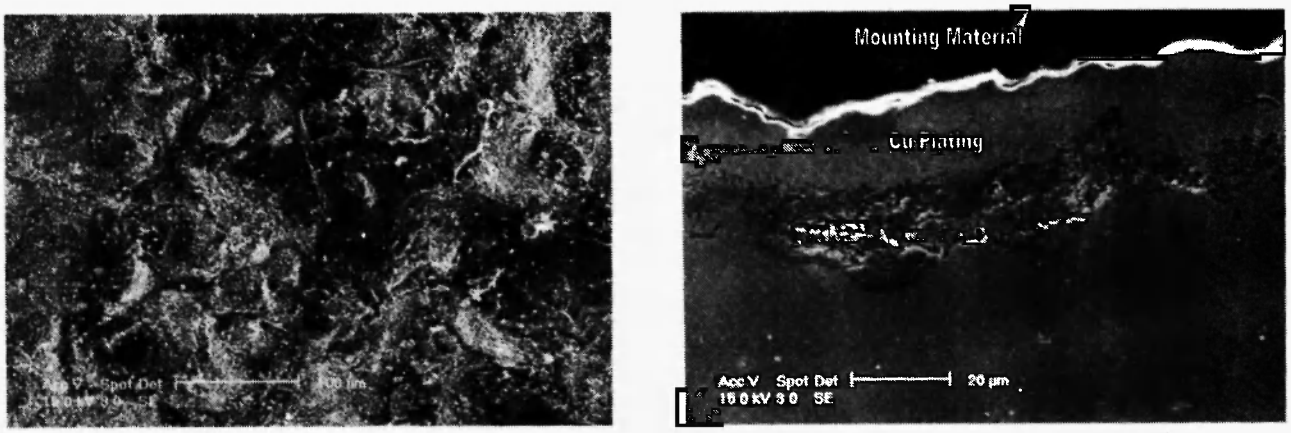

(a) (b)

Fig. 7: Surface morphologies and cross-sections of un-coated and coated stainless steel specimens after oxidation: (a, b) un-coated 304S.S at 1000°C for 100h; (c, d) 304S.S coated with Al at 1000°C for 100h; (e, f) 304S.S coated with FeCrAl at 1000°C for 100h; (g, h) 304S.S coated with FeCrAl+Y_2O_3 at 1000°C for 100h; (i) un-coated 430S.S at 900°C for 100h; (j) 430S.S coated with Al at 900°C for 100h; (k,l) un-coated 310S.S at 1100°C for 100h; and (m) 310S.S coated with FeCrAl + Y_2O_3 at 1100°C for 100h

Fig 7. continued

(c)

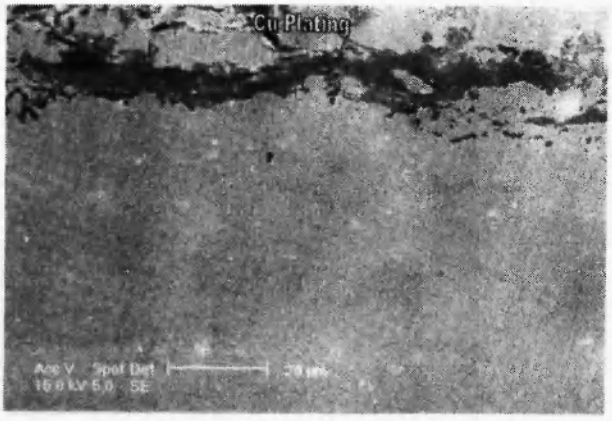

(f)

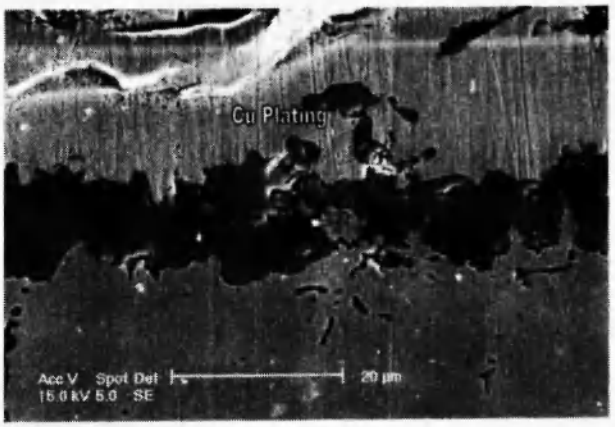

(d)

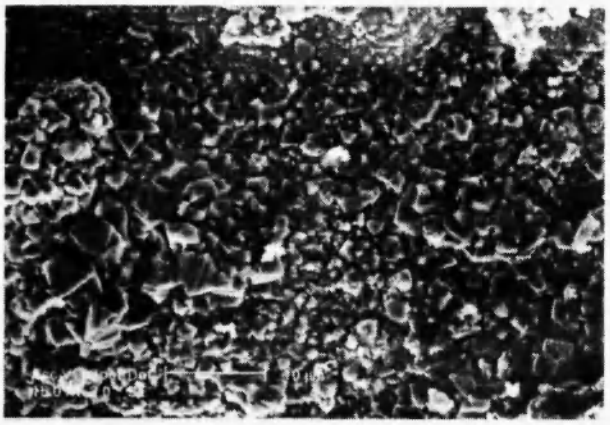

(g)

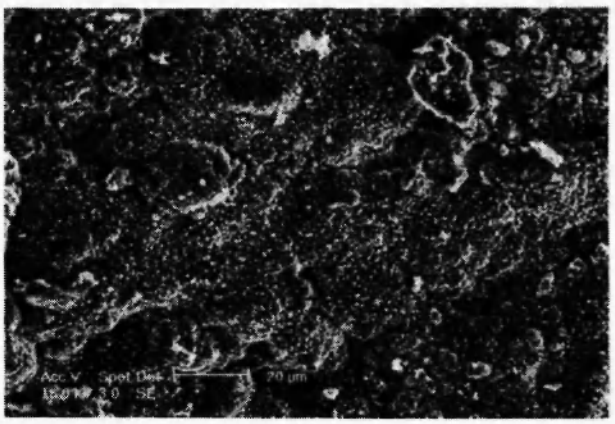

(e)

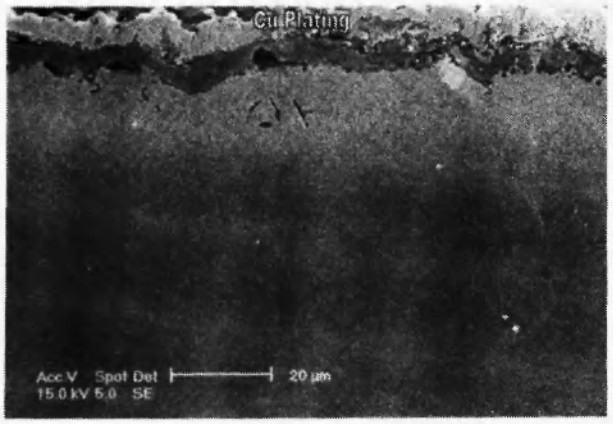

(h)

Fig 7. continued

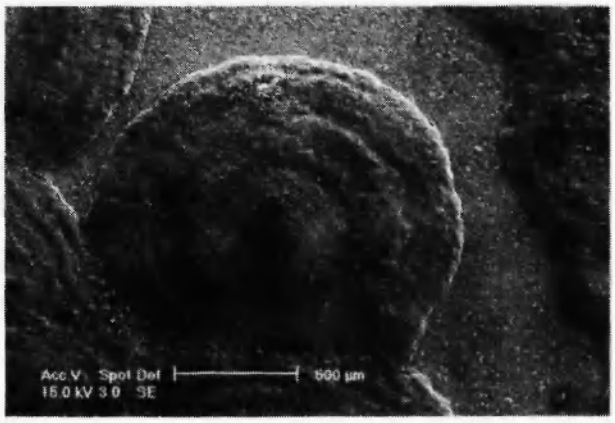

(i)

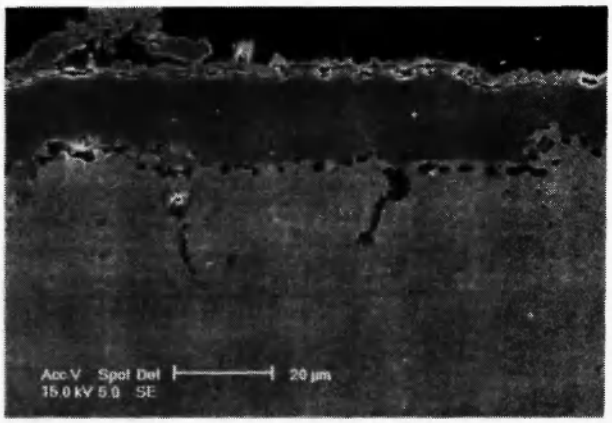

(k)

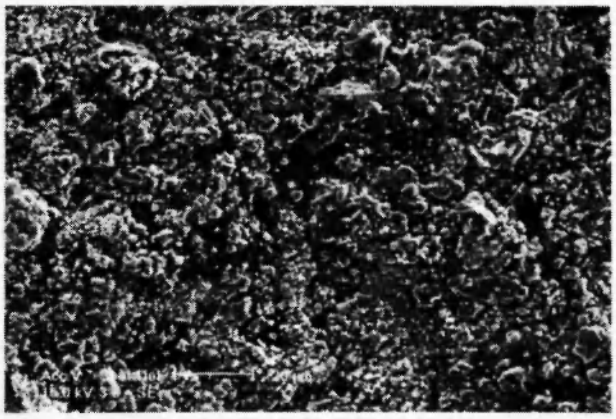

(j)

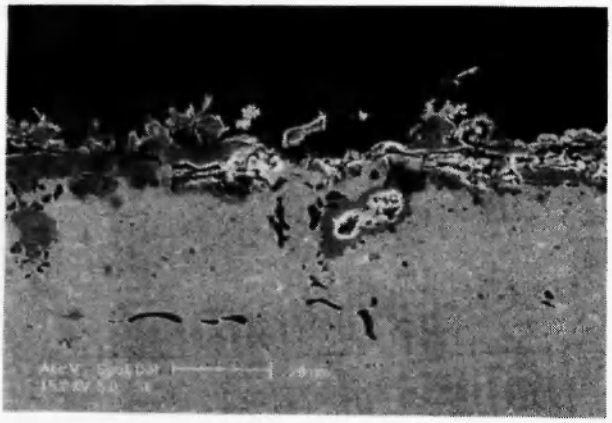

(l)

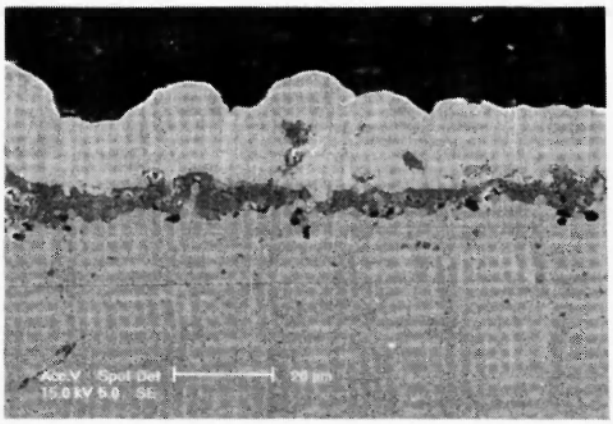

(m)

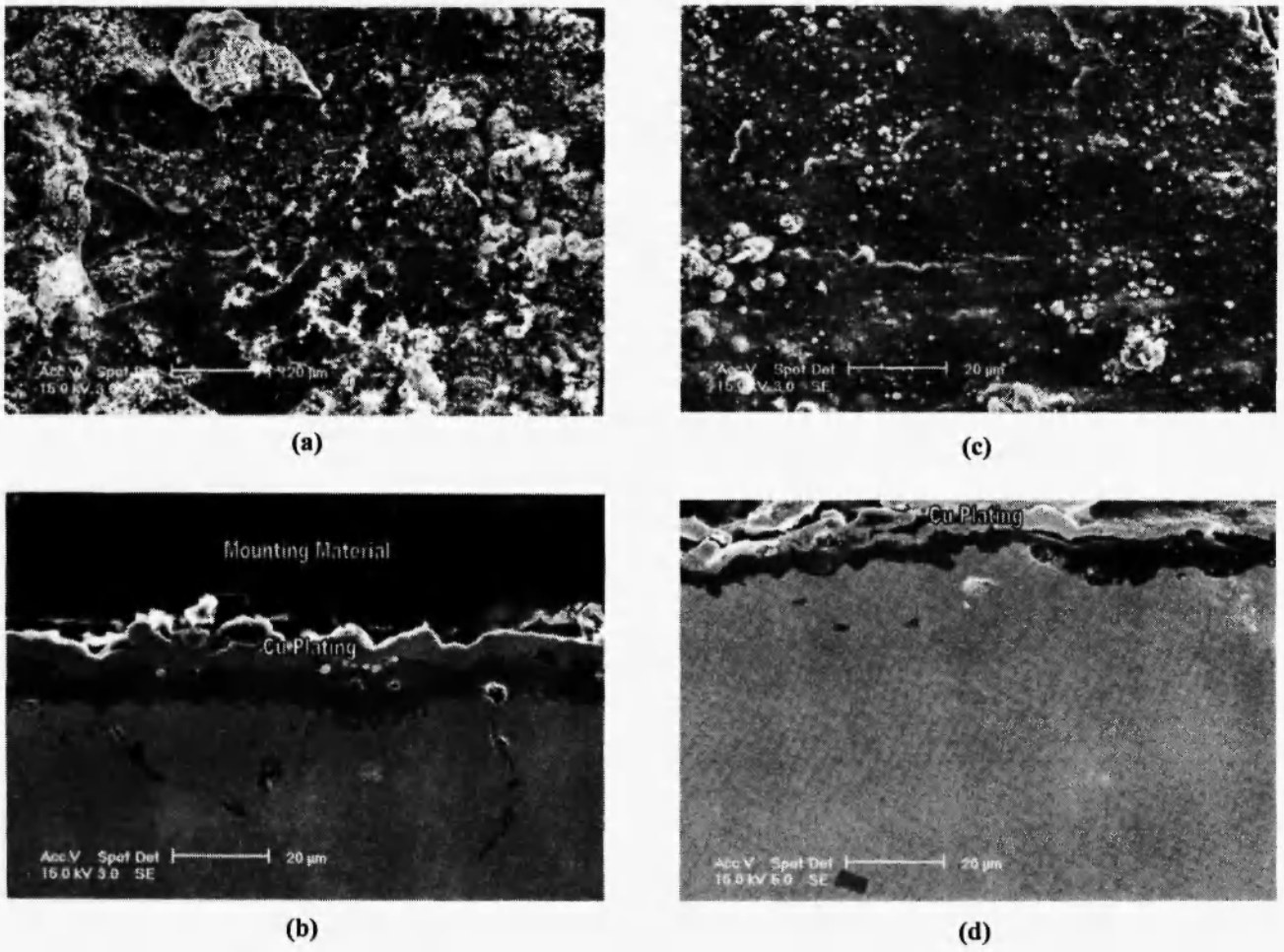

Fig. 8: Surface morphologies and cross-sections of un-coated and coated Inconel 600 alloy specimens after oxidation at 1000°C in air for 200h: (a, b) un-coated Inconel 600; and (c, d) Inconel 600 coated with Al

analysis indicated that this scale mainly consists of Cr, Al and O, although Fe was detected on the top part of the scale.

3.4.2. Un-coated and coated 430S.S

The surface of the un-coated 430S.S after 100h oxidation was covered with two types of oxides: iron oxide (Fe_2O_3 and Fe_3O_4) and spinel oxide ($MnCr_2O_4$), Fig.7 (i). With the formation of thick iron oxides on the surface, the mass of the specimen increased sharply, showing the feature of breakaway oxidation kinetics. Spinel oxides covered the surface of Al-coated 430S.S specimen, Fig. 7 (j). The dark oxide under the spinel was detected as Al oxide.

3.4.3. Un-coated and coated 310S.S

From the polished cross-sections, it can be seen that the oxide scale remaining on un-coated 310S.S was not uniform. Thick scales (>10μm) were formed in some areas, Fig. 7 (k). Serious spallation of scale could be also observed in some other areas, Fig. 7 (l). By contrast, a thin and continuous scale formed on the coated specimen, Fig. 7 (m).

3.4.4. Un-coated and coated Inconel 600 alloy

As for the surface morphologies of Inconel 600 alloy, the coated specimens have more uniform morphologies than the un-coated specimen after oxidation, Fig. 8. While scale spallation can be observed

on the un-coated specimen, fine-grained oxide scale with a small amount of spinel phase formed on the coated specimens. The cross-section micrograph shows that the oxide scale formed on the un-coated alloy consists of two layers: the outer layer of NiO with a small amount of $NiCr_2O_4$, and the inner layer of Cr_2O_3. Deep oxide penetration into the substrate could be seen, Fig.8 (b). Fig.8 (d) shows that α-Al_2O_3 external oxide scale formed on the surface of the alloy coated with Al. These results are consistent with the XRD results.

4. DISCUSSIONS

4.1 Coatings

The technique of electro-spark deposition (ESD) was originally developed for surface hardening and wear resistance. However, the present work shows that it can be used for production of high temperature oxidation resistant coatings.

As the thickness and quality of the coatings are greatly affected by the processing parameters, the effects of the processing parameters on the coating quality should be discussed first. It is understandable that both coating thickness and surface roughness increase with increasing discharge power. The high energy means more coating material is melted and deposited onto the surface during every discharge, and also results in higher surface roughness and micro-defects in the coatings. The detrimental effect of high density of micro-defects on the oxidation behaviour is that more oxygen might transport inward, increasing the oxidation rate. Additionally, if the spark energy is too high, the coating material will be oxidised or nitrided. AlN was occasionally detected on the Al coated 304S.S by XRD.

In a previous study, we reported the effects of spark energy, the frequency of RC circuit and rotating speed of the wheel on the oxidation behaviours of coated specimens. The experimental results indicated that the scale spallation resistance decreases with increasing spark energy level and frequency of the spark under the same wheel rotating rate. The reason for this is probably the increase of micro-defects in the coatings described above. It should be noted that if the rotating speed and the capacitor were kept at constant, an increase in the device frequency means that the circuit can conduct charging more quickly, therefore increasing the charge extent of the capacitor. With higher charge and discharge energy, the coatings produced have higher density of micro-defects. Therefore, to obtain coatings with good oxidation and spallation resistance, a combination of processing parameters must be selected carefully. In the present study, coating operation was conducted twice, the first run with relatively high energy to obtain a coating with a reasonable thickness; the second with low energy for the purpose of uniform and compact coating with smooth surface. It was observed that the coating thickness is a function of both processing parameters and treatment time as the maximum thickness is achieved at different times with different energy /3/. The relation of the coating thickness and deposition time has not been obtained in this work due to the complex processes. However, the speed of the wheel and contact between the wheel and specimen were under careful control because the erosion and abrading of the coating materials by the rotating wheel after repeat treatments were clearly observed.

As an excellent alumina-forming alloy, FeCrAl (especially with Y) can be used as a coating material /9/. In the present study, Fe-25Cr-5Al wire, a commonly used resistance-heating element, was deposited onto 304S.S and 310S.S specimens. In comparison with Al deposition, the contact area between wire and substrate is smaller, and the amount of the coating material deposited in every discharge is also smaller, resulting in more compact and uniform coatings. Because of the flexible nature of the wire, the cutting effect of the rotating wheel on the coatings was modified. A small and flexible contact area is also beneficial to the deposition process on a coarse or small substrate surface, including the specimen edges.

4.2 Oxidation Kinetics

4.2.1 Stainless steels

Stainless steels are the most commonly used structural materials in corrosive environments and at high temperatures. Their oxidation resistance mainly depends on the formation of Cr_2O_3 scale. Cr_2O_3 can be formed on most stainless steels under moderate

oxidising conditions and also on high-Cr stainless steels (e.g., 310S.S) under more severe conditions. However, spinel oxide $FeCr_2O_4$ with less protective ability may also form on low-Cr stainless steels (e.g., 430 or 304S.S). So their usefulness in any given application is governed by the type of oxide scale formed. The recommended maximum temperature for AISI 304, 310 and 430 stainless steels in air for intermittent service is 870, 1035 and 870°C, respectively, and 925, 1150 and 815°C for continuous service /10/, above which catastrophic oxidation takes place. The present oxidation temperatures are much higher than the recommended temperatures. Furthermore, thermal cycling contributes damaging effects, resulting in breakdown oxidation as observed in the present study.

Coating with either Al or FeCrAl showed dramatic improvements to the oxidation/spallation resistance of stainless steels, especially to 304S.S. The total mass gains were reduced, and no obvious spallation was observed. The polished cross-section micrography and XRD results indicated that Cr_2O_3 and α-Al_2O_3 with a small amount of $FeCr_2O_4$ on the top formed on the coated specimens. The formation of Cr_2O_3 and α-Al_2O_3 provided much better oxidation and spallation resistance to stainless steels. However, it should be noted that even on the Al-coated specimen, the oxide scale consists of Cr_2O_3, α-Al_2O_3 and $FeCr_2O_4$, instead of a single phase of α-Al_2O_3. The reasons can be explained as follows:

1. According to the XRD patterns of the Al-coated 304S.S and 430S.S specimens (before oxidation), the coating contains mainly FeAl, but AlN can also be detected with weak peak intensity. FeAl is an excellent alumina-forming alloy /11/ and provides good protective ability as coatings /12/. To a large extent, the formation of this phase in the present coating is beneficial to the oxidation resistance. The formation of AlN, however, is hard to explain on the basis of thermodynamics because the Gibbs energy of formation of AlN is much more positive than that of Al_2O_3. The formation of AlN may be related to the high-energy plasma generated by the spark. The formation of AlN may decrease the amount of Al in FeAl, and also its protectiveness during oxidation.
2. 304S.S and 430S.S do not contain Al. During oxidation at high temperature, Al in the FeAl coatings may diffuse inward into the bulk specimen. This means that the concentrations of Al in the coatings, which are necessary for the formation and growth of Al_2O_3, will be reduced further. As the coating is not thick, Al may drop too low to form and maintain a complete Al_2O_3 scale. However, the Cr concentration in the stainless steels is high (16-18%), the small amount of Al and fine-grained structure (formed due to the rapid solidification process) may play a role of promoting the formation of Cr_2O_3 scale. As for the FeCrAl coatings, the inward diffusion of Al also takes place. It was believed that FeCrAl alloys containing 15-25 wt.%Cr and 4-6 wt.%Al are alumina formers, but alloys containing >13 wt.%Cr and 2-3 wt.%Al are chromina forming alloys /13-17/. So it is believed that the inward diffusion of Al reduced the Al content, resulting in the formation of a scale consisting mainly of Cr_2O_3. As for the FeCrAl+Y_2O_3 coating, the high density dispersion of Y_2O_3 particles in FeCrAl coating may serve as a diffusion barrier to Al /18/, therefore influencing the formation and growth of Al_2O_3, and also the growth of Cr_2O_3 scale /19,20/. These factors are believed to result in the decrease in the oxidation rate compared to the Y_2O_3 free FeCrAl coatings.
3. Micro-pores and micro-cracks could be seen on the coatings, which allow the inward penetration of oxygen. Thus oxidation may take place inside the coatings or at the coating-substrate interface. These factors do not favour the formation of a continuous Al_2O_3 scale. Furthermore, lattice defects in the Cr_2O_3 (+Al_2O_3) scale may also serve as the rapid channel for out diffusion of Fe. The formation of iron oxides or spinel phase also decreases the protective ability of the scales.

4.2.2 Inconel 600 alloy

A continuous, although not very uniform α-Al_2O_3 external scale formed on the Al coated Inconel 600 alloy, providing good oxidation resistance. It is known that aluminising treatment on the surface of Ni or Ni-base alloys improves their resistance to high temperature oxidation /21-23/. Among the Ni-Al alloy

phases (Ni_3Al, Ni_5Al_3, NiAl, Ni_2Al_3 and $NiAl_3$) NiAl phase has the best oxidation resistance /24/. The XRD patterns obtained from the Al coated Inconel 600 specimen showed strong NiAl peaks, evidence of the formation of NiAl phase, which provides good oxidation resistance to the alloy. Furthermore, in comparison with the Fe-based alloys, interdiffusion of Al in Ni is slow. Diffusion of oxygen in Ni is also slower than in α-Fe by 2-3 orders of magnitude at 1000°C /25/. These factors favour the development of a continuous Al_2O_3 scale on the surface.

It is interesting that the kinetic curves of the coated Inconel increased quickly at the beginning, and then levelled off. The mass gain after 10h oxidation is 0.63 mg/cm^2, ~80% of the total mass gain of 200h oxidation. In other words, the oxidation rate of the Al coated Inconel dropped down to a very low level after the initial stage, and kept low for a very long time. This phenomenon can be explained with the phase transformation of Al_2O_3. It was reported that at 1000°C, a distinct transition occurred in the oxidation kinetics of NiAl+Zr alloy. The parabolic rate constant was decreased by two orders of magnitude. This was believed due to the transformation of θ- → α-Al_2O_3 /26/. A transition from γ- to α-Al_2O_3 was reported for the oxide formed during oxidation of NiAl alloy /27/. Due to the fast growth of these metastable alumina phases, the mass gain is high in this stage. It was also reported that the presence of Cr could promote the transformation of γ-Al_2O_3 to α-Al_2O_3 /28/. α-Al_2O_3 may form rapidly and at a relatively low temperature of 900°C for the Al-coated alloys.

The other factors that may cause the high initial oxidation rate include micro-cracks and rough surfaces of the coatings. The micro-defects on the coatings allow the inward diffusion of oxygen. Accelerated oxidation may take place at these locations, resulting in a great mass gain at the early stage. However, as soon as a continuous α-Al_2O_3 forms on the surface, the inward transportation of oxygen is blocked, slowing down the overall growth rate. The spark treated samples have a rougher surface than the untreated samples. This may increase the reaction area substantially. The mass gains were calculated using the specimen geometric area, which is smaller than the real reaction area.

4.3 Scale Spallation Resistance

The greatest improvement of the coatings is in the scale spallation resistance. Scale spallation has complex mechanisms but is generally determined by the properties of the oxides, the interface adherence, and the stresses generation and release in the scales and between the scale and substrate.

For the un-coated 304S.S specimen, the oxides formed are Fe_3O_4 and $FeCr_2O_4$. These two oxides have less protectiveness than Cr_2O_3 and α-Al_2O_3. The high scale growth rate causes high growth stresses, resulting in cracking and detachment of the scales from the substrate, particularly when the scales become thicker (~10μm). Furthermore, rapid temperature changes (which take place during the cooling and heating stages) create high thermal stresses in the oxide layers due to the lower thermal expansion of the oxides. AISI 304S.S is worse than 430S.S because austenitic steels have higher thermal expansion coefficients. For 310 S.S, although $FeCr_2O_4$ and Cr_2O_3 formed, the scale was thick, therefore, the growth stress was relatively high. As for the coated specimens, the oxides scale formed were thin and mainly Cr_2O_3 and α-Al_2O_3. The growth rate was relatively low and so the stresses in the scales.

The electro-spark deposition is a melting/ solidification process in a very short period of time, forming fine-grained coatings. As shown by the SEM images, the oxide grains formed on the coated specimens, especially on FeCrAl (with or without Y_2O_3) coatings, were very small. It is known that the fine oxide grains are beneficial to the high temperature creep of the oxide scales /29/, with which the stresses in the scales can be partially released.

Another explanation is that during the electro-spark deposition operation, the impact applied by the rotating electrode on the sample surface may produce compressive stress and structure defects in the coating surface. Therefore, the surface energy is increased to a higher level that the scale formed can withstand higher elastic deformation caused by the thermal cycling /30/, consequently improving the scale spallation resistance. Additionally, the inward-grown oxide may act as micro-pegs, enhancing the adhesion of the oxide scales to the alloy surface.

4.4 Further Directions for Improvement

The electro-spark coating technique is an efficient surface modification technique. Our results on a number of coatings with various substrates all show significant improvement in oxidation behaviours. The equipment is simple and the operation is fast and not complex. Protective atmospheres can be used but are not necessary. Components with large surface areas and/or irregular shapes can also be treated straight away in ambient air. It can also be used to treat parts and components in-situ, suitable for industrial applications such as surface re-enforce or repair. However, the coating thickness is not uniform and the improvement with different coatings and substrates is different with the preliminary operation conditions. In order to achieve the maximum results, the following improvements should be explored:

1. Increase the coating thickness by using higher energy density;
2. Establish a diffusion barrier on the substrate to prevent the scale forming element from diffusing away;
3. Obtain uniform and dense coatings with less micro-cracks and micro-pores by controlling the processes including the power parameters, moving speed and contact force; and
4. Employ simple but efficient protection against the interaction of reactive elements in the coatings with oxygen or nitrogen in air.

Modification of the equipment and application of this technique for other property improvement is being carried out in our labs.

5. CONCLUSIONS

5.1 Al, FeCrAl (with or without dispersed Y_2O_3 nano-sized particles) coatings were successfully deposited on AISI 304, 310 and 430 stainless steels and Inconel 600 alloy using electro-spark deposition (ESD) technique.

5.2 Oxidation tests in air showed that the coated specimens have dramatically improved resistance to oxidation and scale spallation compared with the un-coated specimens.

5.3 XRD and HRSEM analysis showed that different oxide scales formed on the coated and uncoated specimens. The formation of strong Cr_2O_3 and/or Al_2O_3 scales has contributed to the improvements in oxidation and scale spallation resistance.

ACKNOWLEDGEMENT

This work was supported by New Zealand and Chinese Government Foundations. The authors would also like to thank the Research Centre for Surface and Materials Science and the technical staff in the Department for various forms of support.

REFERENCES

1. T. Burakowski and T. Wierzchon, *Surface Engineering of Metals*, CRC Press, Boca Raton, 1999, chapter.6.
2. N.C. Welsch, *J. Inst. Met.*, **88**, 103 (1959-60).
3. H.U. Stein, in *Science and Technology of Surface Coating*, edited by B.N. Chapman and J.C. Anderson, Academic Press, London and New York, 1974, p129.
4. R.N. Johnson, in *Elevated Temperature Coatings: Science & Technology 1*, edited by N.B. Dahotre, J.M. Hampikian, and J.J. Striglich, The Minerals, Metals & Materials Society, 1995, p265.
5. Z. Huang, *M. Eng. Thesis.*, University of Science & Technology Beijing, March, 1999.
6. Y. He, Z. Huang, H. Qi, D. Wang, Z. Li and W. Gao, "Micro-crystallised Ni-20Cr-Y_2O_3 ODS Alloy Coatings", in print in *Materials Letters*, 11 (1999).
7. Z. Chen, *Electro-Spark Toughening Techniques* (in Chinese), The Mechanical Industry Publishing House, 1985.
8. J. Jedlinski, *Solid State Phenomena*, **21-22**, 335 (1992).
9. M.J. Bennett and S.J. Bull in *Oxidation of Intermetallics*, edited by H.J. Grabke and M. Schütze, Wiley-VCH, Weinheim, 1997, p313 .

10. J.R. Davis, *Heat-Resistant Materials*, ASM International, 1997.
11. R. Prescott and M.J. Graham, *Oxid. Met.*, **38**, 73 (1992).
12. P.F. Tortorelli, I.G. Wright, G.M. Goodwin and M. Howell, in *Elevated Temperature Coatings: Science and Technology 2*, edited by Dahotre and Hampikian, TMS, 1996, p175 .
13. F.H. Stott, G.C. Wood and M.G. Hobby, *Oxid. Met.*, **3**, 103 (1971).
14. F.A. Golightly, F.H. Stott and G.C. Wood, *Oxid. Met.*, **10**, 163 (1976).
15. F.H. Stott, G.C. Wood and F.A. Golightly, *Corro. Sci.*, **19**, 869 (1979).
16. W.J. Quadakkers, K. Schmidt, H. Grübmeier and E. Wallura, *Materials at High Temperature*, **10**, 23 (1992).
17. P. Tomaszewicz and G.R. Wallwork, *Oxid. Met.*, **20**, 75(1983).
18. K.L. Luthra, *J. Vac. Sci. Technol.*, **3A**, 2574 (1985).
19. T.A. Ramanarayanan, R. Ayer, R. Perkovic-Luton and D.P. Leta, *Oxid. Met.*, **29**, 445 (1988).
20. M.J. Bennett and D.P. Moon, in *The Role of Active Elements in the Oxidation Behaviour of High Temperature Metals and Alloys*, edited by E. Lang, Elsevier, London and New York, 1989.
21 G.W. Goward, D.H. Boone and C.S. Giggins, *Trans. ASM.*, **60**, 228 (1967).
22. T.K. Redden, *Trans. AIME.*, **242**, 1695 (1968).
23. G.W. Goward, *J. Metals*, **22**, 31 (1970).
24. T.B. Massalski, *Binary Alloy Phase Diagrams*, 2nd Edition, ASM International, 1992 .
25. T. Yamamoto, T. Takashima and K. Nishida, *Trans. Japan. Inst. Met.*, **21**, 601 (1980).
26. G.C. Rybicki and J.L. Smialek, *Oxid. Met.*, **31**, 275 (1989).
27. W.C. Hagel, *Corrosion*, **21**, 316 (1965).
28. P. Tomaszewicz and G.R. Wallwork, *Rev. High. Temp. Mater.*, **4**, 75 (1978).
29. R.L. Coble, *J. Appl. Phys.*, **34**, 1679 (1963).
30. H.E. Evans, *Int. Mater. Rev.*, **40**, 1 (1995)